LOCALLY ADAPTIVE FUZZY PULMONARY VESSEL SEGMENTATION IN CONTRAST ENHANCED CT DATA

Jens N. Kaftan[ab], Annemarie Bakai[b], Marco Das[c], and Til Aach[a]

[a]Institute of Imaging and Computer Vision, RWTH Aachen University, 52056 Aachen, Germany
[b]Siemens Healthcare Sector, Computed Tomography, 91301 Forchheim, Germany
[c]Department of Diagnostic Radiology, RWTH Aachen University Hospital, 52074 Aachen, Germany

ABSTRACT

Pulmonary vascular tree segmentation is the fundamental basis for different applications, such as the detection and visualization of pulmonary emboli (PE). Such an application requires an accurate and reliable segmentation of pulmonary vessels with varying diameters. We present a novel fuzzy approach to pulmonary vessel segmentation in contrast enhanced computed tomography (CT) data that considers a radius estimate of the current vessel to adapt the segmentation parameters. Hence, our method allows to capture even vessels with small diameters while suppressing leakage into surrounding structures in close proximity of vessels with large diameters. The method has been evaluated on different chest CT scans of patients referred for PE and demonstrates promising results. For quantitative validation, randomly selected sub-volumes that have been semi-automatically segmented by a medical expert have been used as reference to compare the locally adaptive method against the same method with global parameters.

Index Terms— Image segmentation, pulmonary blood vessel, radius estimation, fuzzy connectedness, CT

1. INTRODUCTION

Pulmonary vessel segmentation in CT data is applied in numerous medical applications including detection and visualization of PE and quantitative vessel analysis. Different applications have varying requirements. For example it has been shown in the context of PE detection, that providing a 3D visualization of pulmonary arteries in combination with the traditional 2D examination offers significantly better sensitivity results [1]. Hence it is desirable to segment vessels with varying diameters robustly, since each missed vessel is lost for further diagnostic steps.

Typical segmentation approaches include threshold-based approaches [2], fast marching techniques [3], and fuzzy methods [4]. All these methods have in common that an intensity model of pulmonary vessels is directly or indirectly utilized to detect and delineate the object of interest. However, due to various reasons, e.g., unequal distribution of the used contrast agent and partial volume effects, one can observe that the intensity profile of small vessels significantly differs from that of larger vessels. Consequently, methods using a global intensity model tend to leak into surrounding non-vessel structures in some areas while missing other, particularly smaller vessels (see Fig. 2). We therefore present a method to adapt the expected intensity distribution to the local vessel to be segmented and incorporate it into a fully-automatic segmentation method [4] based on the fuzzy connectedness algorithm [5]. To this end, we estimate the radius of the vessel to be segmented by identifying vessel surface points using a mean shift-based ray propagation technique [6] and use this measure to adapt the segmentation parameters locally. Hence, our method allows to capture vessels with small diameters while suppressing leakage into surrounding structures in close proximity of vessels with large diameters.

The paper is organized as follows. In Section 2 we describe the radius estimation procedure. Subsequently we present the general segmentation algorithm in Section 3. In Section 4, we detail the incorporation of the radius estimate into the segmentation method. We have applied our method to different chest CT scans of patients referred for PE and show segmentation results in comparison to results of the same method with global parameters in Section 5. Finally, we conclude in Section 6.

2. RADIUS ESTIMATION

To estimate the vessel radius at voxel $\mathbf{x}$ within the vessel, rays are cast in different spatial directions. The gray level profiles along these rays of a given length are analyzed to identify vessel surface points (see Section 2.1). Given these points, a principal component analysis (PCA) is applied by determining the eigensystem of the covariance matrix. The radius estimation $\tilde{r}(\mathbf{x})$ can then be computed from the resulting eigenvalues. In general, if $\mathbf{x}$ is located very close to the vessel surface, the identified surface points will be unequally distributed in

We thank Dominik Fritz, Michael Sühling (Siemens Computed Tomography), and André A. Bell (Institute of Imaging and Computer Vision) for their support and helpful discussions.

space, which will reduce the accuracy on the radius estimate. Hence, the results of a first PCA are used to shift $\mathbf{x}$ towards the center of the vessel and the results of a second PCA are then used to determine the radius estimate resulting in a more robust measure.

2.1. Mean shift-based ray analysis

To identify the vessel surface along a 1D ray, one can simply detect the first voxel on the cast ray that is lower than a given threshold T_1 (e.g., $T_1 = 100$ HU). However, it is difficult to find a global threshold because small vessels might appear darker in CT than non-vessel structures in close proximity of large vessels such as airway walls or connective tissue. Hence we seek to identify that point along the ray at which location the intensity profile significantly decreases. For such an objective the mean shift algorithm [7] is very well suited as already shown in [6]. The mean shift procedure smoothes the intensity data along the ray while preserving and sharpening its discontinuities by calculating the mean shift vector

$$\mathbf{m}_K(\mathbf{x}) = \frac{\sum_{i=1}^{N} \mathbf{x}_i K\left(\frac{\mathbf{x}-\mathbf{x}_i}{h}\right)}{\sum_{i=1}^{N} K\left(\frac{\mathbf{x}-\mathbf{x}_i}{h}\right)} - \mathbf{x} \tag{1}$$

for each point until convergence. Then the starting point is assigned with the intensity value of the point of convergence, i.e., the corresponding mode of the probability density function. Here, N equals the number of feature vectors $\mathbf{x}_1, ..., \mathbf{x}_N$ consisting of the 1D spatial and intensity information. The parameter h is the window radius of the used uniform kernel K. To account for different spatial and intensity variances it is reasonable to choose a kernel window with different radii h_s in the spatial and h_r in the intensity domain.

To identify the surface point on the filtered 1D ray, we look for the first significant change in intensity values on the cast ray, which magnitude is larger than a predefined value $\Delta I = I_{\text{before}} - I_{\text{after}} \geq 2 \cdot h_r$. In case such a difference is not observed, the position of the most significant intensity decrease ΔI_{max} is used instead. The results of the mean shift-based boundary detection are exemplarily shown in comparison to the threshold-based variant in Figure 1 using the parameters $h_r = 150$ HU and $h_s = 3$ mm.

3. FULLY-AUTOMATIC PULMONARY VESSEL SEGMENTATION

Our fully-automatic segmentation approach consists of the following steps and has been described in detail in [4]:

1. Lung segmentation
2. Core vessel identification, incl. seed point generation
3. Fuzzy vessel segmentation

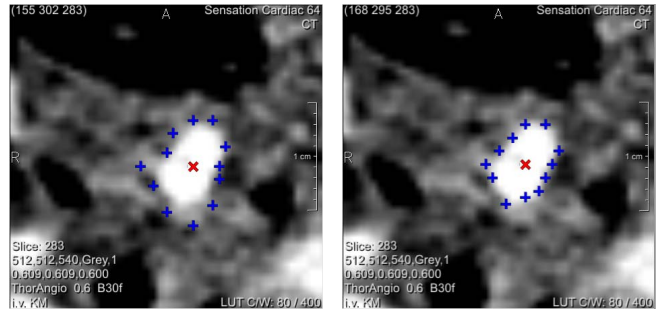

(a) Threshold-based (b) Mean shift-based

Fig. 1. Detected vessel surface points '+' for position 'x' during radius estimation using different ray analysis features.

3.1. Lung Segmentation

There have been different methods proposed to create a lung mask in CT data [2, 3, 8]. We obtain a lung segmentation by starting a region growing from a seed point, automatically selected within the trachea, in order to fill the lungs [2]. To remove the trachea and major airways from the lung mask, a region growing process with adaptive thresholds is started from the trachea seed. Next, morphological closing is performed on the segmented image to fill empty spaces caused by, e.g., blood vessels. Finally, we slightly reduce the size of the lung mask to prevent ribs or other structures near the lung surface from being included in the lung mask.

3.2. Core vessel identification

Based on the masked CT image, we firstly segment the core pulmonary vascular tree using a threshold-based approach. To this end, a lower threshold T_2 is applied and resulting components smaller than a minimum volume V_{min} in size are eliminated. Compared to [2], we choose the parameters in that way that we obtain a core segmentation with a very high specificity, rather than a segmentation of the complete tree structure. Subsequently each component is reduced to one or more seed point by identifying local maxima in a distant transformed image. Depending upon physical location and the distance value, seed points are clustered together such that the cluster representatives tend to be located toward the root of each component. These representatives are then used as seed points for the following step.

3.3. Fuzzy vessel segmentation

The fuzzy segmentation step creates an improved segmentation using the original, masked data along with the identified seed points. Assuming the seed points are located inside the pulmonary vessels the probability that a voxel belongs also to the vascular tree is determined using the fuzzy connectedness algorithm [5].

An object O with its seed points $\mathbf{s}_i$, $i \in [0, n-1]$ and the background B are separated by dividing the set of voxels present in the image volume in such a way that the "belongingness" of each object voxel to the seed points is larger than the "belongingness" of each background voxel.

The probability measure that two neighboring voxels $\mathbf{c}, \mathbf{d}$ belong to the same class or object is therefore defined by a local fuzzy relation called "affinity" $\mu_\kappa(\mathbf{c}, \mathbf{d})$, which is described in detail in Section 4. The "strength of connectedness" of two distant voxels $\mathbf{c}, \mathbf{d}$ along a certain path $p_{\mathbf{c},\mathbf{d}}$ within the image is simply the smallest pairwise local affinity along this path. Here, the path $p_{\mathbf{c},\mathbf{d}}$ from $\mathbf{c}$ to $\mathbf{d}$ is defined as a sequence of $m > 2$ neighboring voxels $\left\langle \mathbf{c}^{(1)}, \mathbf{c}^{(2)}, ..., \mathbf{c}^{(m)} \right\rangle$, such that $\mathbf{c}^{(1)} = \mathbf{c}$ and $\mathbf{c}^{(m)} = \mathbf{d}$. That means, the "strength of connectedness" equals:

$$\mu_N(p_{\mathbf{c},\mathbf{d}}) = \min \left[\mu_\kappa(\mathbf{c}^{(1)}, \mathbf{c}^{(2)}), ..., \mu_\kappa(\mathbf{c}^{(m-1)}, \mathbf{c}^{(m)}) \right] \tag{2}$$

As there are numerous possible paths within the scene, the global connectivity $\mu_K(\mathbf{c}, \mathbf{d})$ is then the largest of the strengths of connectedness of all possible paths between $\mathbf{c}, \mathbf{d}$:

$$\mu_K(\mathbf{c}, \mathbf{d}) = \max_{p_j \in \mathbb{P}_{\mathbf{c},\mathbf{d}}} \left[\mu_N(p_j) \right] \quad \forall\, j \tag{3}$$

where $\mathbb{P}_{\mathbf{c},\mathbf{d}}$ denotes the set of all possible paths p_j. The probability that a voxel $\mathbf{x}$ belongs to a vessel is hence:

$$P_{\text{Vessel}}(\mathbf{x}) = \max_{\mathbf{s}_i} \left[\mu_K(\mathbf{x}, \mathbf{s}_i) \right] \quad \text{with} \quad P_{\text{Vessel}}(\mathbf{s}_i) = 1 \;\; \forall\, i \tag{4}$$

Note that even if P_{Vessel} drops below 0.5 for a voxel, this voxel can still most likely belong to the vascular tree. In fact, an appropriate threshold has to be chosen for binarization.

4. LOCALLY ADAPTIVE AFFINITY

The local affinity $\mu_\kappa(\mathbf{c}, \mathbf{d})$ in Section 3.3 describes the likelihood that a voxel belongs to the class "vessel" and that two neighboring voxels $\mathbf{c}, \mathbf{d}$ belong to the same class, respectively. It has been shown in [4] that using an intensity-based probability function will generally yield good segmentation results:

$$\mu_\kappa(\mathbf{c}, \mathbf{d}) = \begin{cases} e^{-\frac{1}{2\sigma_1^2}\left(\frac{I(c)+I(d)}{2} - \mu_1\right)^2} & \text{if} \quad \frac{I(c)+I(d)}{2} < \mu_1 \\ 1 & \text{else} \end{cases} \tag{5}$$

with $I(\mathbf{c})$ being the intensity value at position $\mathbf{c}$ and μ_1, σ_1^2 being the expected intensity value and variance of the used Gaussian function. The expected intensity value is estimated from the input data by averaging the intensity values of all seed points $\mathbf{s}_i$ while the variance is set to a defined value ($\sigma_1 = 150$) that provided the best results in an empirical study. However, one can observe that using such a probability function with global parameters tends to assign a larger probability measure P_{Vessel} to non-vessel structures in close proximity to vessels with larger diameters than to small vessels itself (see Fig. 2). The reason is that small vessels might appear darker than, e.g., connective tissue or airway walls due to various reasons such as partial volume effects and inhomogeneous contrast agent distribution. To avoid such behavior we incorporate a radius estimation (see Section 2) into the segmentation approach in that way, that we adapt the segmentation parameters based on the radius estimate at the current voxel position. In particular, we increase the variance parameter with decreasing radius estimate using a linear function

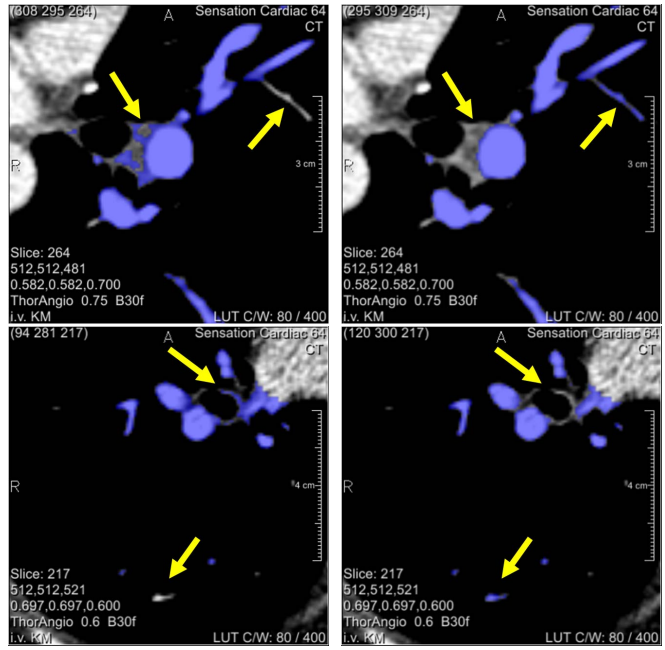

(a) Global parameters (b) Adaptive parameters

Fig. 2. Segmentation results using the proposed method on two different patients. Using global parameters (a) will cause the segmentation process to leak into non-vessel structures while missing small vessels. These vessels are accurately segmented using the adaptive approach (b).

$$\sigma_{\text{adaptive}} = \begin{cases} \sigma_{\min} & \tilde{r}(\mathbf{x}) > \mu_{\tilde{r}} \\ \sigma_{\max} & \tilde{r}(\mathbf{x}) < \tilde{r}_{\min} \\ \sigma_{\min} + (\mu_{\tilde{r}} - \tilde{r}(\mathbf{x})) \cdot \frac{\sigma_{\max} - \sigma_{\min}}{\mu_{\tilde{r}} - \tilde{r}_{\min}} & \text{else} \end{cases} \tag{6}$$

with $\sigma_{\min}$ being the minimal value for σ that results in an accurate segmentation of larger vessels, e.g., $\sigma_{\min} = 100$, and $\sigma_{\max}$ being the maximal value, which equals the constant parameter setting ($\sigma_{\max} = \sigma_1$). Additionally, $\mu_{\tilde{r}}$ equals the average radius estimation of all seed points $\mathbf{s}_i$ and $\tilde{r}_{\min}$ the minimal radius estimate for which the segmentation parameters are adapted ($\tilde{r}_{\min} = 2$mm).

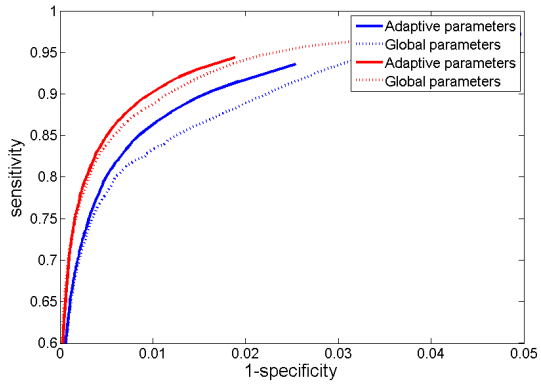

Fig. 3. Quantitative segmentation results for two patients.

5. RESULTS

The proposed method has been evaluated on five different contrast enhanced chest CT scans from clinical routine of patients referred for PE and demonstrates promising results (see Fig. 2). These data have been acquired using Siemens Sensation 16/64 scanners with voxel sizes ranging from 0.55-0.7 mm in x, y and 0.6-0.7 mm in z-direction. For quantitative validation 30 manually selected regions of interests (ROI) have been semi-automatically segmented using a combination of automatically, threshold-based created fore- and background seed points in combination with the random walker algorithm [9], which has demonstrated to yield accurate results applicable for validation purposes [10]. For each patient, six randomly placed ROIs (two close to the hilum and four within the periphery of the lung) of size 50^3 voxels have been used as ground truth. The adaptive method demonstrates an improved segmentation for all cases. The resulting receiver operating characteristics (ROC) for varying thresholds for P_{Vessel} are exemplarily shown in Figure 3. It can be seen that the sensitivity (ratio of truly positive segmented voxels to all object voxels) increases up to 5% at constant specificity (ratio of truly negative segmented voxels to all background voxels) (blue curves). In some cases, however, the performance of both methods is almost equivalent (red curves).

6. CONCLUSIONS

We have described a fully automatic approach to pulmonary vessel segmentation in contrast enhanced CT data using the fuzzy connectedness method. One can observe that segmentation methods using global parameters typically leak into non-vessel structures in close proximity to larger vessels before capturing small vessels. Hence, we locally adapt the segmentation parameters of our fuzzy approach based on a radius estimation method. Using this adaptive method exhibits promising results based on a semi-automatically segmented ground truth. We could show that the proposed adaptive method is able to capture more small vessels while reducing leakage into non-vessel structures than a non-adaptive method. However, calculating the radius estimate for every considered voxel increases the processing time significantly (from approx. 30s to 150s for a typical dataset with a given lung segmentation on a Intel®Core™2 CPU with 2.13GHz). In the future we therefore plan to group voxels and to estimate the radius value only once for each group. Additionally the chosen relationship between radius estimate and segmentation parameters will be examined in more detail on a larger database.

7. REFERENCES

[1] A. P. Kiraly, C. L. Novak, D. P. Naidich, I. Vlahos, J. P. Ko, and G. T. Brusca-Augello, "A comparison of 2D and 3D evaluation methods for pulmonary embolism detection in CT images," in *SPIE Medical Imaging*, Mar. 2006, vol. 6146, pp. 132–140.

[2] A. P. Kiraly, E. Pichon, D. P. Naidich, and C. L. Novak, "Analysis of arterial subtrees affected by pulmonary emboli," in *SPIE Medical Imaging*, May 2004, vol. 5370, pp. 1720–1729.

[3] T. Buelow, R. Wiemker, T. Blaffert, C. Lorenz, and S. Renisch, "Automatic extraction of the pulmonary artery tree from multi-slice CT data," in *SPIE Medical Imaging*, Apr. 2005, vol. 5746, pp. 730–740.

[4] J. N. Kaftan, A. P. Kiraly, A. Bakai, M. Das, C. L. Novak, and T. Aach, "Fuzzy pulmonary vessel segmentation in contrast enhanced CT data," in *SPIE Medical Imaging*, Feb. 2008, vol. 6914, 69141Q.

[5] J. K. Udupa and S. Samarasekera, "Fuzzy connectedness and object definition: theory, algorithms, and applications in image segmentation," *Graph. Models Image Process.*, vol. 58, no. 3, pp. 246–261, 1996.

[6] H. Tek, D. Comaniciu, and J. P. Williams, "Vessel detection by mean shift based ray propagation," in *IEEE Workshop on Mathematical Methods in Biomedical Image Analysis. MMBIA*, 2001, pp. 228–235.

[7] D. Comaniciu and P. Meer, "Mean Shift Analysis and Applications," in *International Conference on Computer Vision. ICCV*, 1999, vol. 2, pp. 1197–1203.

[8] S. Hu, E. A. Hoffman, and J. M. Reinhardt, "Automatic lung segmentation for accurate quantitation of volumetric x-ray ct images," *IEEE Transactions on Medical Imaging*, vol. 20, no. 6, pp. 490–498, June 2001.

[9] L. Grady, "Random walks for image segmentation," *IEEE Transactions on Pattern Analysis and Machine Intelligence*, vol. 28, no. 11, pp. 1768–1783, 2006.

[10] J. N. Kaftan, A. Bakai, F. Maier, and T. Aach, "Semi-automatic pulmonary vessel segmentation in CT data as reference to validate automatic approaches (German)," in *Bildverarbeitung für die Medizin*, 2008, to appear.